Design principles of cell circuits with paradoxical components

Yuval Hart[a], Yaron E. Antebi[b], Avraham E. Mayo[a], Nir Friedman[b], and Uri Alon[a,1]

Departments of [a]Molecular Cell Biology and [b]Immunology, Weizmann Institute of Science, Rehovot 76100, Israel

Edited by Daniel S. Fisher, Stanford University, Stanford, CA, and accepted by the Editorial Board March 23, 2012 (received for review November 5, 2011)

Biological systems display complex networks of interactions both at the level of molecules inside the cell and at the level of interactions between cells. Networks of interacting molecules, such as transcription networks, have been shown to be composed of recurring circuits called network motifs, each with specific dynamical functions. Much less is known about the possibility of such circuit analysis in networks made of communicating cells. Here, we study models of circuits in which a few cell types interact by means of signaling molecules. We consider circuits of cells with architectures that seem to recur in immunology. An intriguing feature of these circuits is their use of signaling molecules with a pleiotropic or paradoxical role, such as cytokines that increase both cell growth and cell death. We find that pleiotropic signaling molecules can provide cell circuits with systems-level functions. These functions include for different circuits maintenance of homeostatic cell concentrations, robust regulation of differentiation processes, and robust pulses of cells or cytokines.

T helper cells | IL-2 | Tregs | TGF-β | IL-27

Gene regulation networks are composed of a handful of recurring circuit elements, called network motifs (1). Theory and experiments have shown that each network motif can carry out specific dynamical functions in an autonomous way, such as filtering noisy signals, generating output pulses, and speeding responses (1).

Here, we ask whether one can apply this approach to the level of circuits made of interacting cells. For this purpose, we consider cells that communicate by means of secreted molecules. These secreted molecules affect cell behaviors such as rate of proliferation and cell death. Previous studies on such cell systems attempted to include many cell types and interactions in a model involving numerous biochemical parameters and variables (2–5). Other works focused on the effects of a single cell type responding, for example, to a ligand that it secretes itself; these works showed the interplay between cell to cell variability and positive feedback, leading to bistability (selection), formation of thresholds for immune response, and memory (6, 7).

Here, we study simple models of circuits made of a few communicating cell types. Because many of the interactions in cell circuits are poorly characterized at present, we seek models in which the exact functional form of the interactions does not affect the conclusions; therefore, models have a degree of generality. We also scan all possible topologies with a given set of components to obtain the widest class of circuits that can perform a given function.

We consider circuit designs that seem to recur in immunology. An intriguing feature of these systems is the fact that many secreted signaling molecules (cytokines) are pleiotropic: they have multiple effects, sometimes antagonistic or paradoxical, such as increasing both proliferation and death of a certain cell type. We find that pleiotropic signals, in the configurations suggested by immune circuits, can provide circuits with specific dynamical functions. We discuss several such functions—homeostatic cell concentrations, robust regulation of differentiation processes, and robust pulses of cells or cytokines—and the corresponding immune circuit examples. The predicted functions can be readily tested experimentally.

Results

Fundamental Features of Cell Circuits. We consider models of cells that interact using chemical signals, such as cytokines, which we will denote generally as ligands. Cells can divide to form new cells of the same type, differentiate to new cell types, secrete ligands, and take up ligands from the medium. Cells are removed by cell death, migration, or differentiation. We define cell circuits as collections of interacting cells that perform specific dynamical functions.

To understand cell circuits, it is useful to study simple models of their dynamics. In this section, we introduce notation and equations as a basis for the following sections. The dynamics of the concentration of cells of type X can be described using a first-order differential equation (Eq. **1**):

$$\dot{X} = \beta X - \alpha X, \qquad [1]$$

where α is the cell removal rate, and β is its proliferation rate. The rate of new cell production, βX, is proportional to X, because all cells arise from existing cells by cell division. Eq. **1** results in a sensitive situation: if $\beta < \alpha$, X tends to zero, whereas if $\beta > \alpha$, X tends to infinity (Fig. 1*A*).

Note that nonlinear terms can be added to Eq. **1** to prevent cell concentrations from diverging to infinity. For example, a nonlinear proliferation rate that decreases as cells approach a limiting concentration [e.g., $\beta X(1 - X/X_{max})$] limits the population at the maximal carrying capacity X_{max}, in which available volume or other limiting factor runs out. In the present study, we seek mechanisms that can stabilize cell concentrations at values much smaller than the carrying capacity of the body or organ in question.

Eq. **1** stands in contrast to the typical equation of molecular circuits, where molecule m is produced at rate β and removed at rate α (1, 8, 9). The difference is that the production rate of molecules is usually zero order (β rather than βm). Thus (Eq. **2**),

$$\dot{m} = \beta - \alpha m, \qquad [2]$$

which has a nonzero stable steady state $m_{st} = \beta/\alpha$ without need for additional regulation (Fig. 1*B*). Specific molecular circuits can show bistability (1, 8, 9), but these circuits require a special design, such as positive feedback or autocatalysis such that $\beta = \beta(m)$ is a function of m over some range.

The intrinsic instability of Eq. **1** raises the need for regulation of cell proliferation and removal rates. One mode of regulation involves the response of cells to a ligand, with concentration that is denoted by c. When ligand is produced by cells X and acts on proliferation and removal rates β and α in Eq. **1**, feedback mechanisms can arise. Below, we discuss simple cell circuits that can carry out such feedback.

An additional fundamental process is differentiation, where cell type X_0 gives rise to a different cell type X_1, and therefore (Eq. **3**),

Author contributions: Y.H., Y.E.A., A.E.M., N.F., and U.A. designed research, performed research, analyzed data, and wrote the paper.

The authors declare no conflict of interest.

This article is a PNAS Direct Submission. D.S.F. is a guest editor invited by the Editorial Board.

[1]To whom correspondence should be addressed. E-mail: urialon@weizmann.ac.il.

This article contains supporting information online at www.pnas.org/lookup/suppl/doi:10.1073/pnas.1117475109/-/DCSupplemental.

$$\dot{X}_1 = \beta X_0 - \alpha X_1. \quad [3]$$

This simple situation results in dynamics of X_1 that depend on the initial concentration of precursor cells X_0 (Fig. 1*C*). One may expect that concentrations of precursors vary from individual to individual and in the same individual over time, raising the challenge of making the response of the system insensitive to such fluctuations (10–13).

For the sake of simplicity, in the following analysis, we consider only the average cell dynamics, and therefore, no spatial component (7, 14) or stochastic components (6, 15) of the diversity between cells are included. Such factors can be readily added in future studies.

Homeostatic Cell Concentration with an OFF State by Ligand Enhancement of both Proliferation and Removal Rates. As mentioned above, achieving a specified cell concentration requires control of proliferation and/or removal rates. We now discuss ways in which such regulation can be achieved.

Consider a cell type X that produces ligand c that affects the cell's proliferation rate $\beta(c)$ and its removal rate $\alpha(c)$. The production–removal equation is (Eq. **4**)

$$\dot{X} = (\beta(c) - \alpha(c))X, \quad [4]$$

where c is produced by X (Eq. **5**):

$$\dot{c} = \beta_2 X - \gamma\, c. \quad [5]$$

Eqs. **4** and **5** have a form known as integral feedback (16, 17). They allow a nonzero steady state only at a special ligand level c^*, at which proliferation rate equals removal rate $\beta(c^*) = \alpha(c^*)$.

The way in which $\beta(c)$ and $\alpha(c)$ depend on c is important for the behavior of the circuit. We consider here the situation found in $CD4^+$ T-cell proliferation, where the cytokine c = IL-2 produced by these cells is a pleiotropic signal for both their proliferation and death (18, 19). In this system, both β and α increase with c (Fig. 2 *A* and *B*).

When β and α both increase as a function of c and cross each other with appropriate slopes, a stable steady-state solution is found, c^*, as shown graphically in Fig. 2*D*. Furthermore, when ligand is not present ($c = 0$), the cell population goes to a second fixed point (an OFF state) with no cells, $X = 0$ (because X derivative in time equals zero for $X = 0$; Eq. **4**).

Because X produces the ligand c, Eq. **5** implies that steady state occurs at a unique value of the cell concentration (Eq. **6**):

$$X^* = \frac{\gamma}{\beta_2} c^*. \quad [6]$$

This steady-state cell concentration X^* (and ligand concentration c^*) is independent of the initial number of cells $X(t = 0)$ for a wide range of $X(t = 0)$ values in the basin of attraction of the ON state (Fig. 2*C*). Thus, a stable nonzero steady state is achieved, which contrasts the simple circuit designs with no regulation described above (Fig. 1*A*). At very low initial cell levels, the cell number decays to zero—the OFF state (Fig. 2*C*). The stable OFF state ensures that small fluctuations do not cause a full response.

Other possibilities, such as one rate decreasing with c and one rate increasing with c levels, abolish either the stability of the OFF state or the stability of the ON state (Fig. 2 *E* and *F*, respectively). These considerations constrain the possible dependence of β and α on c.

These predictions can be readily tested experimentally by using different initial levels of T_h-effector cells and following their proliferation curves over time (similar to Fig. 2*C*) to test whether differentiated cell levels are insensitive to precursor levels. Indeed, several studies have shown, using adoptive transfer experiments, that precursor amounts are weakly correlated with final levels of differentiated cells (10–13) (*SI Appendix*). For example, Badovinac et al. (10) found that, over a four order of magnitude change of precursor amounts, the change in total effector $CD8^+$ T cells is less than one-half an order of magnitude. Recent theoretical explanations rely on negative feedback mechanisms, which can provide partial compensation for precursor levels (20, 21) (additional discussion in *SI Appendix*).

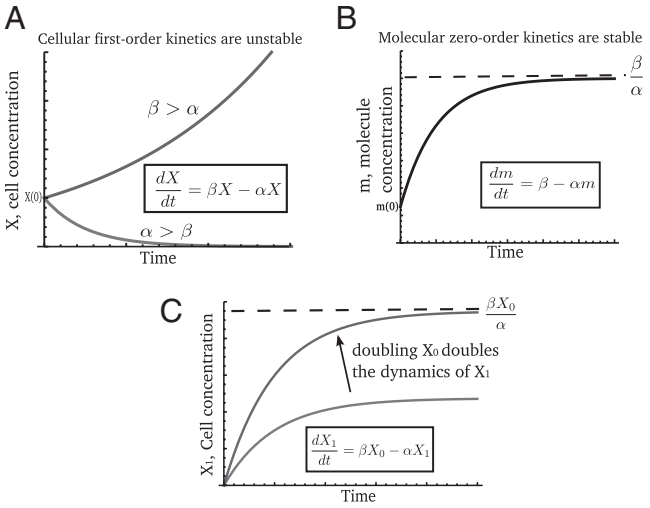

Fig. 1. Without special regulation, cell concentration dynamics are inherently unstable and sensitive to precursor cell levels, whereas dynamics of molecular circuits are stable. (*A*) Dynamics of cell concentration where cell proliferation rate is β and removal rate is α. (*B*) Dynamics of molecule concentration produced at rate β and removed at rate α reach a unique, stable steady state. (*C*) Dynamics of cells X_1 that differentiate from a precursor population X_0 at rate β and are removed at rate α with no divisions.

Analysis of All Circuit Topologies with One Cell Type and One Ligand Shows a Small Class of Mechanisms for Stable Cell Concentrations with an OFF State. To test the generality of the above mechanism, we studied all possible circuits with one cell type X and one ligand c. In each circuit topology, cells X proliferate and are removed and they can uptake and/or secrete c. The ligand c affects cell proliferation and/or death rates, and it can be produced by X and/or an external source. Models that include all of these effects are (Eq. **7**)

$$\dot{X} = (\beta(c) - \alpha(c))X \quad [7]$$

and (Eq. **8**)

$$\dot{c} = \beta_3 + \beta_2 X - \alpha_0 X f(c) - \gamma(c), \quad [8]$$

where β_3 is the external c source, $\beta_2 X$ is c secretion rate by X, the term with α_0 is the rate of uptake of c by X, and $\gamma(c)$ is the rate of c degradation. Note the use of general functional forms that are assumed only to be smooth and monotonic.

One can omit some of the processes in Eqs. **7** and **8**, resulting in different circuit topologies. Each circuit topology is defined by which of the six terms in Eqs. **7** and **8** is present, yielding a total of 24 topologies that are connected in the sense that c affects X and X affects c in some way (Fig. 3*A*). We find that 15 of 24 topologies can yield a stable steady-state solution in which X equals $X^* > 0$ (*SI Appendix*, Fig. S1). Stability conditions can be derived analytically (*Methods*), resulting in inequalities to be satisfied by the various functions in Eqs. **7** and **8**. This analysis shows that the circuits are stable for a wide range of functional forms and parameters. The origin of the stable fixed point in all of these circuits is an effective negative feedback loop (1, 8, 9), in which increase in cell numbers leads to a change in c that reduces cell numbers.

We also asked which of the circuits can show both a stable ON state and a stable OFF state. We find that this feature requires that ligand c affects both proliferation and death, which occurs in 4 of the 24 circuits (marked in Fig. 3*A*). To have both states, assuming that X and c positively correlate, $\beta(c) - \alpha(c)$ needs to have negative values for low and high c levels, while being positive for midvalues

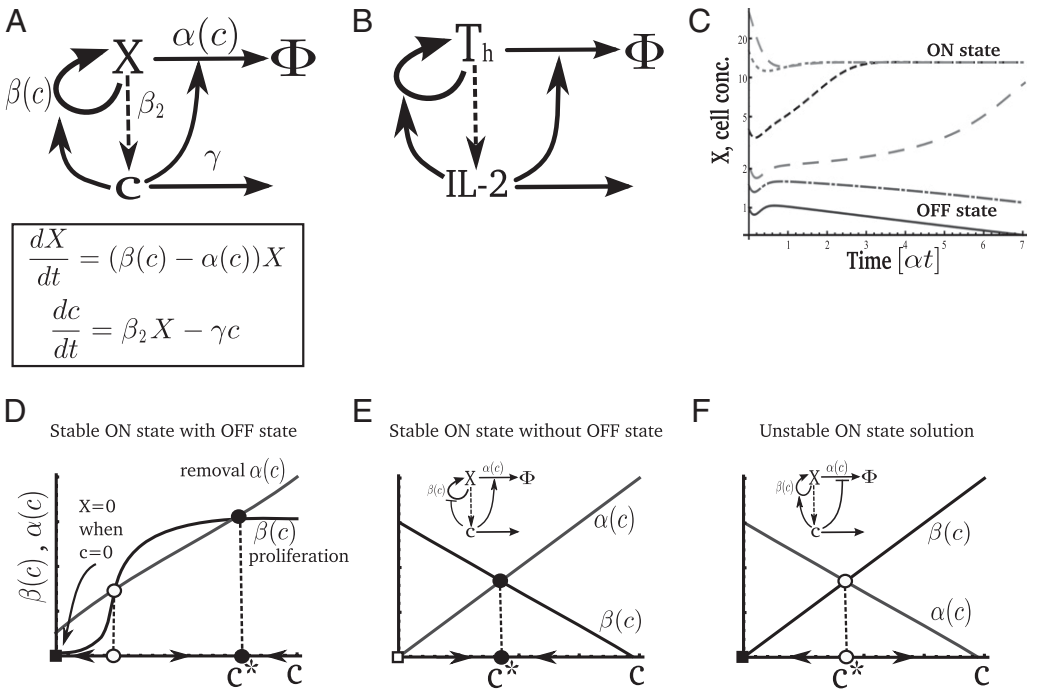

Fig. 2. Cytokine control can provide a homeostatic concentration of cells and an OFF state at low initial cell levels. (*A*) Schematic of a circuit in which cytokine *c* is produced by cells *X* at rate β_2 and degraded at rate γ. The cytokine affects both the cell proliferation rate $\beta(c)$ and the removal rate $\alpha(c)$. (*B*) An immune example of this circuit, where T_h cells produce IL-2, which increases both their proliferation rate and apoptotic rate. (*C*) Above a certain threshold in initial cell levels, cell concentration dynamics of circuit (*A*) converge to a unique steady state (the ON state) independent of initial amounts of *X* or *c*. At low initial cell levels, cell concentration dynamics decay to zero (the OFF state). Here, $\alpha(c) = c$, $\beta(c) = 3\frac{c^2}{c^2+1}$, $\beta_2 = 1$, $\gamma = 5$, $c(0) = 5$, and $X(0) = 1$, 1.5, 2, 4, 16, and 32. (*D–F*) For *X* to be in steady state, its time derivative needs to be zero. There are two ways this can happen: either $X = 0$ or $\beta(c) = \alpha(c)$ (Eq. **4**). In *D–F*, circles denote fixed points caused by crossing of $\beta(c)$ and $\alpha(c)$, whereas squares denote fixed points caused by $X = 0$ without such a crossing (the OFF state). The latter occurs when $c = 0$. Full circles and squares mark stable fixed points; open circles and squares mark unstable ones. (*D*) When cell proliferation and removal rates both increase with *c* and cross each other with appropriate slopes, a stable steady-state solution is found, $c^* > 0$. In addition, when $c = 0$, the cell population goes to a second stable fixed point (an OFF state) with no cells, $X = 0$. (*E*) When cytokine *c* inhibits proliferation rate and enhances removal rate, a single stable steady state occurs without a stable OFF state. (*F*) When cytokine c inhibits removal rate and enhances proliferation rate, the steady-state ON state solution is unstable.

of *c*. This situation occurs, for example, when both $\beta(c)$ and $\alpha(c)$ are increasing functions of *c* and cross each other, like in the functions $\alpha(c) = c$ and $\beta(c) = \frac{3c^2}{c^2+1}$ used in Fig. 2*C*. In other words, the ligand should be paradoxically pleiotropic, increasing both proliferation and removal of cells (*SI Appendix* has a general analysis of the fixed points and their stability). In these circuits, the cell concentration at the ON state, X*, can be tuned by changing the external source of the ligand, β_3. The origin of the stable OFF state is an effective positive feedback loop on top of the negative loop required for the stable ON state (8, 9). These two loops are enabled by the paradoxical nature of the ligand.

An analysis of the phase plane dynamics of these circuits is presented in *SI Appendix*, showing that some of them can show a pulse of *c* production, whereas others have monotonic *c* dynamics (*SI Appendix*, Fig. S1).

To summarize, 4 of 24 possible circuit topologies can show a stable steady-state cell level with both ON and OFF states. One of these circuit topologies seems to appear in the $CD4^+$ T-cell system (Fig. 2*B*). All four topologies use a paradoxically pleiotropic ligand.

Differentiated Cell Concentration That Is Robust to the Precursor Cell Concentration. Next, we consider a situation in which cell type X_1 is continuously produced from precursor cells X_0. The aim is a circuit that can make the concentration of X_1 independent of the concentration of precursor cells X_0 and yet responsive to an input ligand *c*. Such a circuit can make X_1 insensitive to naturally occurring fluctuations in the level of the precursor cell population.

We begin with a simple circuit based on an immunological system. Then, we analyze all circuit topologies with a precursor cell type and a differentiated cell type that interact with one ligand.

Consider a circuit (inspired by an immunological example described below) in which the ligand *c* increases the rate at which the precursor cell X_0 differentiates to cell type X_1 (Eq. **9**):

$$\dot{X}_1 = \beta_0 f(c) X_0 - \alpha X_1. \qquad [9]$$

Here, $f(c)$ is an increasing function of *c* that describes signaling that occurs when *c* binds its receptors on X_0 cells, stimulating differentiation. The precursor cells X_0 in this circuit have a second role: they inhibit the ligand by taking it up (by endocytosis). Thus, the ligand removal rate depends on X_0. Because endocytosis of a ligand or cytokine typically involves its binding to the same receptors that it uses for signaling (22, 23), one can make the important assumption that the uptake rate per cell is proportional to the signaling rate per cell (Eq. **10**)

$$\dot{c} = \beta_3 - \alpha_1 f(c) X_0. \qquad [10]$$

Note that the same function $f(c)$ appears in both Eqs. **9** and **10** because of the linked biological mechanisms of signaling and endocytosis (23).

As a result, at steady state, Eq. **10** shows that the ligand reaches a level c^* such that $f(c^*)$ is inversely proportional to X_0, $f(c^*) = \frac{\beta_3}{\alpha_1 X_0}$. Plugging this result into Eq. **9** shows that the steady-state concentration of X_1 is independent of X_0:

$$X_1^* = \frac{\beta_0 \beta_3}{\alpha \alpha_1}. \qquad [11]$$

This behavior stands in contrast to simpler designs, in which the differentiated cell levels increase with precursor cell levels (Fig. 1*C*). Intuitively, X_1^* is independent of precursor concentration because the precursors X_0 have two antagonistic roles: they are both the source of X_1 and at the same time, the inhibitor of the stimulatory ligand *c* (Fig. 4). These two effects cancel out the dependence of X_1 on X_0: more X_0 means a proportional increase in both production of X_1 and inhibition of *c*.

This principle may apply to the differentiation of $CD4^+$ T cells (X_0) into effector cells such as T_h2 cells (X_1) in response to the input ligand c = IL-2. In the initial stages of differentiation relevant for the present discussion, IL-2 is found in low but stimulatory levels. The cytokine IL-2 communicates an immune challenge and results in increased levels of helper T cells. At the same time, there exists a second population, regulatory T cells

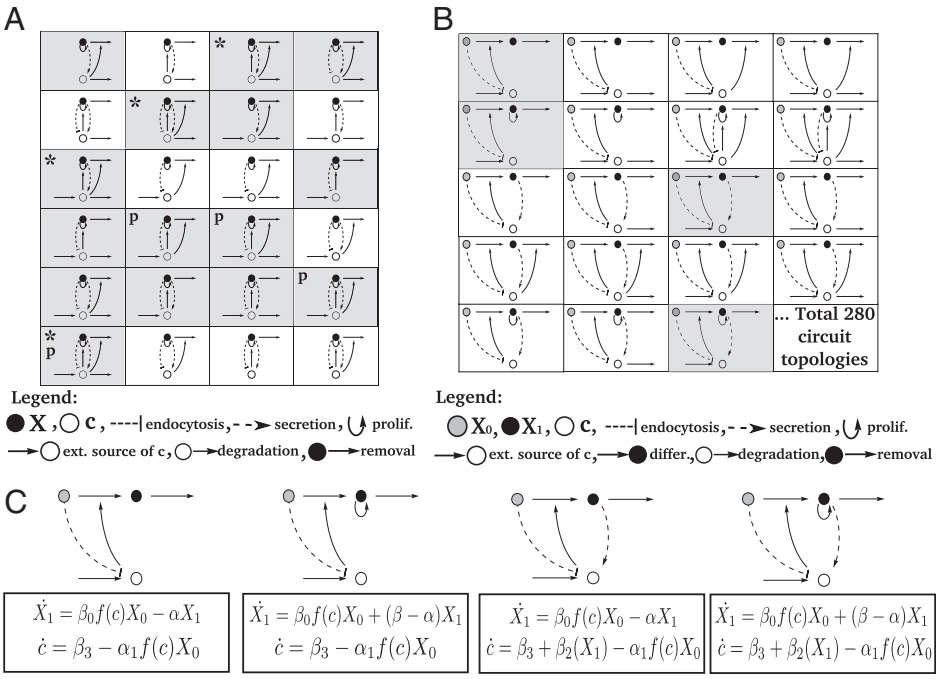

Fig. 3. Analysis of circuit topologies that yield homeostatic cell concentrations. (*A*) All 24 connected topologies with a single cell type and a ligand; 15 of 24 topologies can show steady-state cell levels that are independent on initial levels (highlighted in gray). Circuits marked with a star show both ON and OFF stable states. Circuits marked with p show a pulse in ligand levels. (*B*) A sample of the 280 connected topologies of a two-cell differentiation process controlled by a single ligand. The four topologies highlighted yield a steady-state differentiated cell level that is independent on the precursor cell level. (*C*) The four topologies highlighted in *B* and their corresponding model equations.

(Tregs). This cell population is roughly proportional to the concentration of $CD4^+$ T cells (ranging between 5% and 10% of the $CD4^+$ T cells) (24). Tregs complete the circuit by taking up IL-2 by endocytosis using the same IL-2 receptors that bind IL-2 to stimulate differentiation of $CD4^+$ T-cells (6, 7, 25). This system was recently modeled by Busse et al. (7), including its spatial organization, showing that Tregs compete for IL-2; thus, their levels set a threshold for the immune response. In the present context, we find that this circuit (Fig. 4) leads to a steady-state level of helper T cells that is independent of the amount of precursors but responsive to the level of input signal through the parameter β_3. This result can be readily tested experimentally by varying precursor $CD4^+$ T-cell concentration and monitoring the helper T-cell response to a given stimulus (Fig. 4*C*).

Only a Small Number of Circuit Topologies with a Differentiation Process and One Ligand Show Robust Differentiated Cell Levels. To test the generality of the above mechanism, we considered all circuit topologies with two cell types: a precursor X_0 that differentiates into cell type X_1 and one ligand. The ligand can be secreted and endocytosed by either or both cell types and/or externally produced or degraded. The ligand affects X_0 differentiation rate, X_1 proliferation, and/or death rate. In all circuits, we assume that endocytosis rate is proportional to the signaling rate by the ligand as discussed above.

In total, there are 280 such connected topologies (19 of which are shown in Fig. 3*B*). Of these, we find that only four topologies show a stable steady-state concentration of differentiated cells X_1, which is independent on X_0 concentration (*SI Appendix*, Fig. S2). These topologies are highlighted in Fig. 3*B*. The circuit topology of the previous section is one of these four topologies. The other three topologies differ in the absence or presence of X_1 proliferation and in the source of c, allowing for production of c by X_1.

These four circuit topologies show that the two antagonistic roles of the precursor cells—creating X_1 cells and at the same time, inhibiting the ligand—are essential for achieving homeostasis of differentiated cells in the present class of models.

The mathematical reason for the independence of X_1 on X_0 in these mechanisms, discussed in *SI Appendix*, is that a variable composed of a combination of X_1 and c shows integral feedback. *SI Appendix* also discusses additional topologies that have X_1 independent of X_0 but require specific functional forms for the interactions (such as linear forms).

Cell Circuits That Can Provide Pulse-Like Dynamics of Cells or Cytokines. We conclude with two examples of circuits that can produce pulse-like dynamics. The function of these circuits depends on specific mathematical forms for some of the interactions. The first circuit, based on the incoherent feedforward loop (IFFL) design (1), produces a pulse of cells in response to a step-like stimulus rather than a prolonged response. In this sense, it shows sensory adaptation (8, 26). Furthermore, in a certain parameter range, this circuit can sense fold changes (relative changes) in input ligand rather than absolute changes (27–29) (Fig. 5*C*).

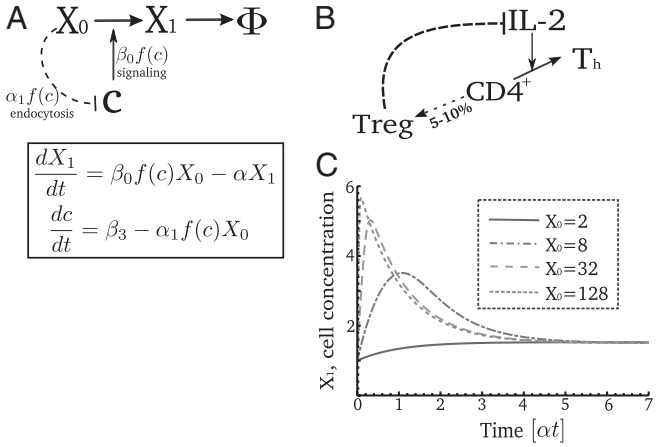

Fig. 4. A circuit that produces a robust amount of differentiated cells by endocytosis of a cytokine by the precursor cells. (*A*) Schematic of a circuit in which cytokine c enhances the differentiation of X_1 cells from precursor cells X_0. The precursors also remove c by endocytosis. (*B*) An example of the circuit in differentiation of T-helper cells: $CD4^+$ cells differentiation to T-helper cells (e.g., Th2 cells) is enhanced by IL-2. However, Treg cell level is roughly proportional to the $CD4^+$ pool (5–10% of $CD4^+$ levels; proportionality is marked as a dotted arrow). Tregs take up IL-2, thus reducing its levels. (*C*) Dynamics of X_1 cell concentration reach a homeostatic steady state that is independent of the levels of precursors X_0. Different lines represent different X_0 levels (contrast with Fig. 1*C*). Here, $\alpha = \beta_0 = 1$, $\beta_3 = 3$, $\alpha_1 = 2$, $f(c) = c/c + 3$, $X_1(0) = 1$, and $c(0) = 10$.

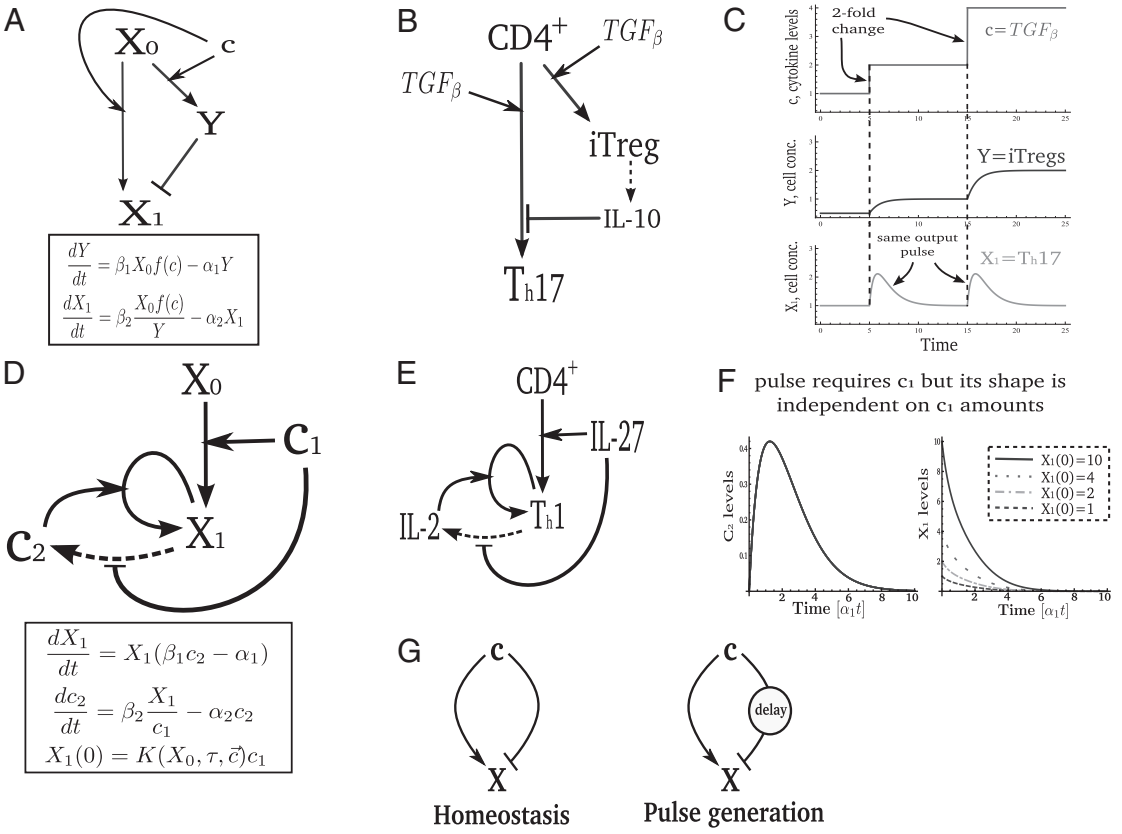

Fig. 5. Cell circuits that produce a robust pulse of cells or cytokines. (*A*) An incoherent feed-forward loop of cells with a shared cytokine. (*B*) An example in which c = TGF_β enhances the differentiation of X_0 = $CD4^+$ T cells to X_1 = T_h17 cells and Y = iTreg cells. iTreg cells inhibit the differentiation of $CD4^+$ T cells to T_h17 by secreting IL-10. Note that iTregs also secrete TGF_β but at later times, after the dynamics considered here are over. (*C*) For a wide range of parameters, this cell circuit model can display fold-change detection and exact adaptation. The circuit generates a pulse of T_h17 cell levels in response to a change in TGF_β levels. The same fold change in TGF_β leads to the same pulse dynamics, regardless of absolute TGF-β, a feature known as fold-change detection. Here, $\alpha_1 = \beta_1 = \beta_2 = \alpha_2 = 1$, $X_0 = 1$, $X_1(0) = 1$, and $Y(0) = 0.25$. (*D*) A circuit that produces a pulse of output signal with shape and size that is independent on the triggering input signal strength. Precursor cells X_0 differentiate to X_1 cells when triggered by cytokine c_1 (the input). This differentiation is completed at an early time, and therefore, initial X_1 level [$X_1(0)$] for the second proliferative stage depends on the levels of precursors cell X_0, the differentiating cytokine c_1, τ (the duration of the first differentiation stage), and $\vec{c}$ (other differentiation-activating cytokines in the environment). At later times, X_1 proliferates and secretes the output signal c_2, which enhances X_1 proliferation. The input cytokine c_1 inhibits production of c_2 (dynamic equations for X_1 and c_2 at the second stage are shown). (*E*) An example of the circuit: c_1 = IL-27 promotes X_1 = T_h1 differentiation but also inhibits T_h1 secretion of c_2 = IL-2. IL-2 is secreted by T_h1 and increases its proliferation rate. (*F*) The circuit dynamics show that, although (*Right*) X_1 levels depend on c_1 levels (different marking for each level), (*Left*) the shape and size of the dynamic pulse of c_2 levels are independent of c_1 or X_0 levels (all trajectories align). Here, $\alpha_1 = \beta_1 = \beta_2 = \alpha_2 = 1$, $c_1 = 1$, 2, 4, and 10, $X_1(0) = c_1$ [i.e., $K(X_0, \tau, \vec{c}) = 1$], and $c_2(0) = 0$. (*G*) Design principle for components with paradoxical pleiotropy in cellular and molecular circuits.

A possible example of such a circuit occurs in the context of T_h17 cell differentiation (Fig. 5*B*). The paradoxical pleiotropy here is that TGF_β induces differentiation to two cell types with opposing effects (T_h17 and iTregs) (30, 31).

Finally, we consider a cell circuit that can produce a pulse of secreted cytokine (the output) in response to an input cytokine. The special feature of this circuit is that the output pulse depends on the presence of the input, but its shape (including amplitude and decay time) are independent on the amount of the input cytokine. In the circuit, the input cytokine c_1 causes precursor cells X_0 to differentiate into X_1 cells. X_1 cells produce the output cytokine c_2, which increases their own proliferation rate. The input cytokine c_1 is pleiotropic in that it inhibits the production of c_2 by X_1. The equations in Fig. 5 describe the circuit using first-order terms for c_1 and c_2. Note that this architecture differs from the IFFL, which is also a pulse-generating circuit (1, 32), because it includes a feedback loop (X_1 produces c_2, which enhances X_1 proliferation).

The dynamics of the output c_2 are pulse-like in response to addition of c_1 (Fig. 5*F* and extended analysis in *SI Appendix*). The elements of this circuit are found in the IL-27–dependent differentiation of T_h1 cells (Fig. 5*E*). The paradoxical role of IL-27 was initially discovered when knockout of the IL-27 receptor in T_h1 cells caused an unexpected T-cell hyperactivity (33).

Discussion

This study explored circuits made of communicating cells that display specific dynamical functions. These functions include formation of stable homeostatic cell concentrations with an OFF state, differentiated cell levels that are independent on precursor cell concentration, and circuits that generate pulses of cells or cytokines. The function carried out by each circuit depends on the specific architecture of its interactions and especially on components which have paradoxical or opposing effects. The models in many of the cases do not depend on the exact functional form of the interactions. We also provided examples from the immune system that seem to have the elements of each circuit type.

The biological functions discussed here might be useful in the immune system and also in other contexts, such as development. Homeostatic amounts of differentiated cells (Figs. 2–4) allow for a response that resists fluctuations in precursor cell amounts and initial cell amounts. This mechanism provides a precise steady-state cell concentration, which can also be tuned by ligand signals. In the immune system, this mechanism can help overcome variations in the number of lymphocytes responding to a given antigen, variations in

sizes of lymph nodes, or variations in the amounts of predifferentiated cells. In the context of development, such circuits might help maintain a desired concentration of a cell type in a growing organ, independent of the precursor cell population.

Fold-change detection mechanisms (Fig. 5) can provide cell circuits with features analogous to well-studied sensory systems ranging from the visual and auditory system to bacterial chemotaxis (26, 27). Responding to fold changes rather than absolute change allows for detecting signals above noisy backgrounds and filtering out variations that multiply the input by a constant, such as variations in cell numbers and other parameters (27).

The last mechanism considered here for creating a robust, stereotyped pulse response (Fig. 5) can allow a precise dose of output cytokine, despite fluctuations between individuals (such as different lymph node volumes). Because cytokines are potent regulators of cell functions, their secretion must be carefully regulated. The present mechanism allows a sizable response, with amplitude that is not too large or too small, avoiding the deleterious effects of immune hyperactivity. Such stereotyped pulse-like doses seem to occur in the context of pulsing transcription factors (34, 35) such as p53 in response to DNA double-stranded breaks, where pulse amplitude and shape are independent on signal level (36). A similar situation may also occur in hormone pulses (26) and might also be relevant for neurotransmitter production.

The present study provides a functional explanation of why many cytokines have paradoxically opposite effects on different processes. We find that such paradoxical components can provide cell circuits with useful biological functions: homeostasis (robustness) and pulse generation.

A principle that emerges is that paradoxical components may have one of two general effects depending on whether the functions carried out by the component act at the same time or at a delay (Fig. 5*G*). When there is no delay, antagonistic pleiotropy helps maintain homeostasis (Figs. 2 and 4). When there is a delay, it produces a robust pulse output (Fig. 5). This principle applies also to molecular circuits: bifunctional enzymes can lead to homeostasis by carrying out antagonistic functions at the same time (37–39), and IFFLs lead to pulses by carrying out antagonistic functions at a delay.

The present analysis includes the simplest considerations of population averages without taking space into account. Additional work can examine the effects of cell–cell variability (e.g., in receptor numbers), stochastic effects in sensing, and the effects of the spatial distribution of cells and ligands (7, 14). Spatial organization can be important, because the combined effect of ligand diffusion and uptake creates a microenvironment of limited extent in which a given cell can affect its neighbors (7, 14). The present models make specific predictions for experiments, in which certain dynamics are expected to be insensitive to varying cell or cytokine concentrations.

More generally, it would be interesting to map additional principles from the level of molecular circuits to the level of circuits of interacting cells. Cell circuits may provide building blocks to understand complex cellular networks.

Methods

To analyze the fixed point stability of Eqs. **7** and **8**, we calculated the Jacobian (J) and asked when the determinant and trace obey Det(J) > 0 and Tr(J) < 0. The following inequalities should hold for the different fixed points to be stable. The point $X = 0$, $c = \frac{\beta_3}{\gamma} = c_0$ is stable when $\beta(c_0) < \alpha(c_0)$. When $\beta_3 = 0$, then $c_0 = 0$, and the condition sets proliferation to be lower than removal rate at zero ligand concentration, making the OFF state stable. The ON state fixed point $X = X^*$, $c = c^*$ is stable when $-(\beta'(c^*)) - \alpha'(c^*))(\beta_2 - \alpha_0 f(c^*)) > 0$, which means that either $\beta'(c^*) > \alpha'(c^*)$ and $\beta_2 < \alpha_0 f(c^*)$ or $\beta'(c^*) < \alpha'(c^*)$ and $\beta_2 > \alpha_0 f(c^*)$ (*SI Appendix*).

ACKNOWLEDGMENTS. U.A. is the incumbent of the Abisch-Frenkel Professorial Chair. U.A. thanks the European Research Council (FP7) and the Israel Science Foundation for support. N.F. is the incumbent of the Pauline Recanati Career Development Chair of Immunology. N.F.'s research was supported by the International Human Frontier Science Program Organization.

1. Alon U (2007) Network motifs: Theory and experimental approaches. *Nat Rev Genet* 8:450–461.
2. Goldstein B, Faeder JR, Hlavacek WS (2004) Mathematical and computational models of immune-receptor signalling. *Nat Rev Immunol* 4:445–456.
3. Zheng H, et al. (2008) How antigen quantity and quality determine T-cell decisions in lymphoid tissue. *Mol Cell Biol* 28:4040–4051.
4. Ishii M, et al. (2009) Sphingosine-1-phosphate mobilizes osteoclast precursors and regulates bone homeostasis. *Nature* 458:524–528.
5. Chakraborty AK, Das J (2010) Pairing computation with experimentation: A powerful coupling for understanding T cell signalling. *Nat Rev Immunol* 10:59–71.
6. Feinerman O, et al. (2010) Single-cell quantification of IL-2 response by effector and regulatory T cells reveals critical plasticity in immune response. *Mol Syst Biol* 6:437.
7. Busse D, et al. (2010) Competing feedback loops shape IL-2 signaling between helper and regulatory T lymphocytes in cellular microenvironments. *Proc Natl Acad Sci USA* 107:3058–3063.
8. Tyson JJ, Chen KC, Novak B (2003) Sniffers, buzzers, toggles and blinkers: dynamics of regulatory and signaling pathways in the cell. *Curr Opin Cell Biol* 15:221–231.
9. Ferrell JE, Jr., et al. (2009) Simple, realistic models of complex biological processes: positive feedback and bistability in a cell fate switch and a cell cycle oscillator. *FEBS Lett* 583:3999–4005.
10. Badovinac VP, Haring JS, Harty JT (2007) Initial T cell receptor transgenic cell precursor frequency dictates critical aspects of the CD8(+) T cell response to infection. *Immunity* 26:827–841.
11. Hataye J, Moon JJ, Khoruts A, Reilly C, Jenkins MK (2006) Naive and memory CD4+ T cell survival controlled by clonal abundance. *Science* 312:114–116.
12. Whitmire JK, Benning N, Whitton JL (2006) Precursor frequency, nonlinear proliferation, and functional maturation of virus-specific CD4+ T cells. *J Immunol* 176:3028–3036.
13. Quiel J, et al. (2011) Antigen-stimulated CD4 T-cell expansion is inversely and log-linearly related to precursor number. *Proc Natl Acad Sci USA* 108:3312–3317.
14. Shvartsman SY, Wiley HS, Deen WM, Lauffenburger DA (2001) Spatial range of autocrine signaling: Modeling and computational analysis. *Biophys J* 81:1854–1867.
15. Deenick EK, Gett AV, Hodgkin PD (2003) Stochastic model of T cell proliferation: A calculus revealing IL-2 regulation of precursor frequencies, cell cycle time, and survival. *J Immunol* 170:4963–4972.
16. Barkai N, Leibler S (1997) Robustness in simple biochemical networks. *Nature* 387: 913–917.
17. Yi T-M, Huang Y, Simon MI, Doyle J (2000) Robust perfect adaptation in bacterial chemotaxis through integral feedback control. *Proc Natl Acad Sci USA* 97:4649–4653.
18. Refaeli Y, Van Parijs L, London CA, Tschopp J, Abbas AK (1998) Biochemical mechanisms of IL-2-regulated Fas-mediated T cell apoptosis. *Immunity* 8:615–623.
19. Li XC, et al. (2001) IL-15 and IL-2: A matter of life and death for T cells in vivo. *Nat Med* 7:114–118.
20. Bocharov G, et al. (2011) Feedback regulation of proliferation vs. differentiation rates explains the dependence of CD4 T-cell expansion on precursor number. *Proc Natl Acad Sci USA* 108:3318–3323.
21. Kim PS, Lee PP, Levy D (2010) Emergent group dynamics governed by regulatory cells produce a robust primary T cell response. *Bull Math Biol* 72:611–644.
22. Gesbert F, Sauvonnet N, Dautry-Varsat A (2004) Clathrin-Independent endocytosis and signalling of interleukin 2 receptors IL-2R endocytosis and signalling. *Curr Top Microbiol Immunol* 286:119–148.
23. Di Fiore PP, De Camilli P (2001) Endocytosis and signaling. an inseparable partnership. *Cell* 106:1–4.
24. Sakaguchi S (2004) Naturally arising CD4+ regulatory t cells for immunologic self-tolerance and negative control of immune responses. *Annu Rev Immunol* 22:531–562.
25. Pandiyan P, Zheng L, Ishihara S, Reed J, Lenardo MJ (2007) CD4+CD25+Foxp3+ regulatory T cells induce cytokine deprivation-mediated apoptosis of effector CD4+ T cells. *Nat Immunol* 8:1353–1362.
26. Keener JP, Sneyd J (1998) *Mathematical Physiology* (Springer, Berlin).
27. Shoval O, et al. (2010) Fold-change detection and scalar symmetry of sensory input fields. *Proc Natl Acad Sci USA* 107:15995–16000.
28. Goentoro L, Shoval O, Kirschner MW, Alon U (2009) The incoherent feedforward loop can provide fold-change detection in gene regulation. *Mol Cell* 36:894–899.
29. Ma W, Trusina A, El-Samad H, Lim WA, Tang C (2009) Defining network topologies that can achieve biochemical adaptation. *Cell* 138:760–773.
30. Li MO, Flavell RA (2008) Contextual regulation of inflammation: A duet by transforming growth factor-β and interleukin-10. *Immunity* 28:468–476.
31. McGeachy MJ, Cua DJ (2008) Th17 cell differentiation: The long and winding road. *Immunity* 28:445–453.
32. Basu S, Mehreja R, Thiberge S, Chen M-T, Weiss R (2004) Spatiotemporal control of gene expression with pulse-generating networks. *Proc Natl Acad Sci USA* 101:6355–6360.
33. Villarino A, et al. (2003) The IL-27R (WSX-1) is required to suppress T cell hyperactivity during infection. *Immunity* 19:645–655.
34. Lahav G, et al. (2004) Dynamics of the p53-Mdm2 feedback loop in individual cells. *Nat Genet* 36:147–150.
35. Süel GM, Garcia-Ojalvo J, Liberman LM, Elowitz MB (2006) An excitable gene regulatory circuit induces transient cellular differentiation. *Nature* 440:545–550.
36. Batchelor E, Loewer A, Lahav G (2009) The ups and downs of p53: Understanding protein dynamics in single cells. *Nat Rev Cancer* 9:371–377.
37. Batchelor E, Goulian M (2003) Robustness and the cycle of phosphorylation and dephosphorylation in a two-component regulatory system. *Proc Natl Acad Sci USA* 100:691–696.
38. Shinar G, Milo R, Martínez MR, Alon U (2007) Input output robustness in simple bacterial signaling systems. *Proc Natl Acad Sci USA* 104:19931–19935.
39. Hart Y, et al. (2011) Robust control of nitrogen assimilation by a bifunctional enzyme in *E. coli*. *Mol Cell* 41:117–127.